

Supporting information

On-demand shape and size purification of nanoparticle based on surface area

Renming Liu,^{‡a} Jian-Hua Zhou,^{‡b} Zhang-Kai Zhou,^{*a} Xueqin Jiang,^b Jiaming Liu,^a Guanghui Liu,^a Xue-Hua Wang^{*a}

^a State Key Laboratory of Optoelectronic Materials and Technologies, School of Physics and Engineering, Sun Yat-sen University, Guangzhou 510275, People's Republic of China

^b Key Laboratory of Sensing Technology and Biomedical Instruments of Guangdong Province, School of Engineering, Sun Yat-sen University, Guangzhou 510275, People's Republic of China

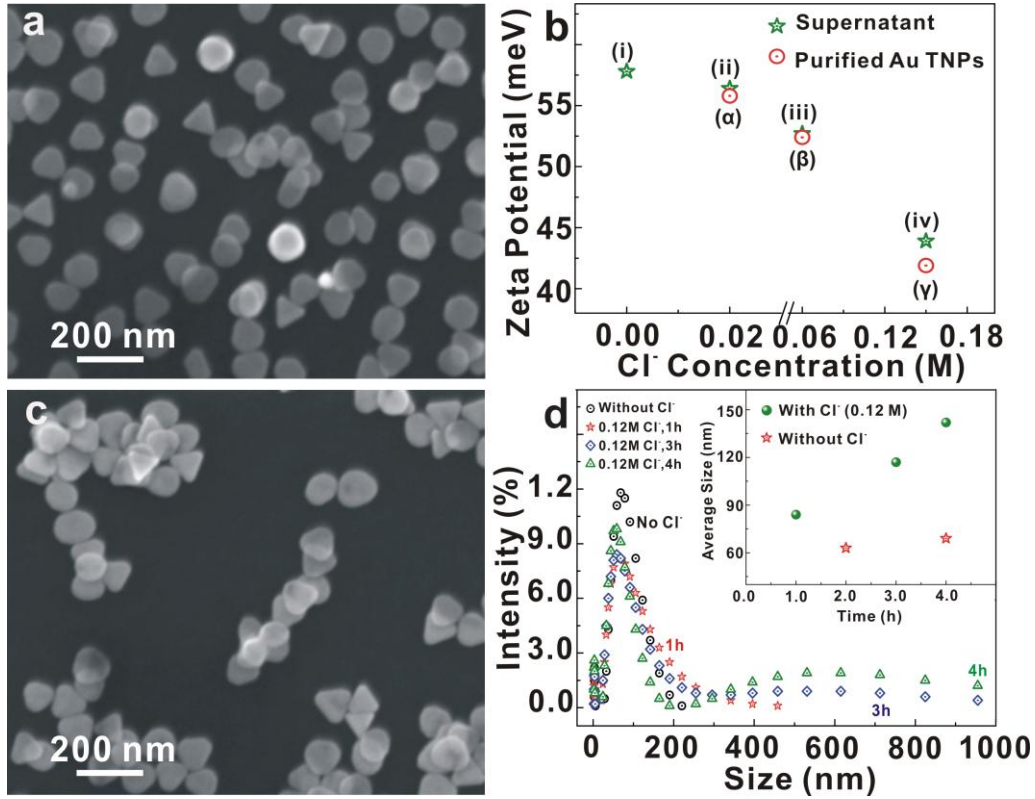


Figure S1. SEM images of the purified Au triangular nanoplates (TNPs) and Zeta potential as well as particle's size distribution of Au nanoparticles (NPs). (a, c) SEM images of purified Au TNPs deposited from the diluted CTAB solutions (5 mM) (a) without Cl^- (the deposition process was terminated after waiting for 12 h) and from the diluted CTAB solutions (5 mM) after adding Cl^- (the final concentration of Cl^- was 0.04 M) for 4 h. (c) Zeta potentials of the NPs in the process of particle's surface area-based separations for Au TNPs. Green stars: Zeta potentials of (i) the mixed Au NPs (including Au TNPs and SNPs), Au NPs in supernatant after (ii) the first, (iii) the second and (iv) the third separation, respectively. Red circles: Zeta potentials of the purified Au TNPs obtained from (α) the first, (β) the second, and (γ) the third purification. (d) Size distributions of the mixed Au NPs (including Au TNPs and SNPs) in CTAB solutions (0.2 M), (black circle) without Cl^- and with addition of Cl^- (0.12 M) after (red star) 1h, (blue diamond) 3h, and (green triangle) 4h. The insert is the average size changes of the particles in CTAB solution (green balls) with and (red stars) without Cl^- along with time.

Note that, Zeta potential $\zeta=4\pi\sigma d/D$, which is proportional to the surface charge density σ . As the Au TNPs and supernatant have nearly the same Zeta potential value, we can consider the σ of these two structures are identical as we do in the theoretical analysis in the Main Text (d is the thickness of electric double layer around the NP's surface, and D is the dielectric constant of the solution).

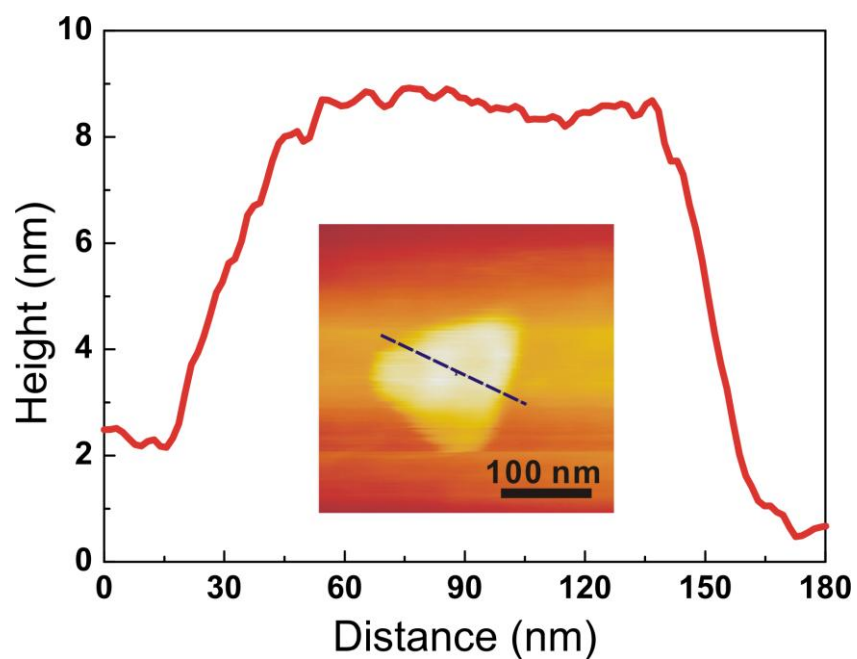


Figure S2. Atomic force microscopy (AFM) image of the Au TNP. The measured thickness is about 7 nm which is in accordance with the result of previous reports.^{1,2}

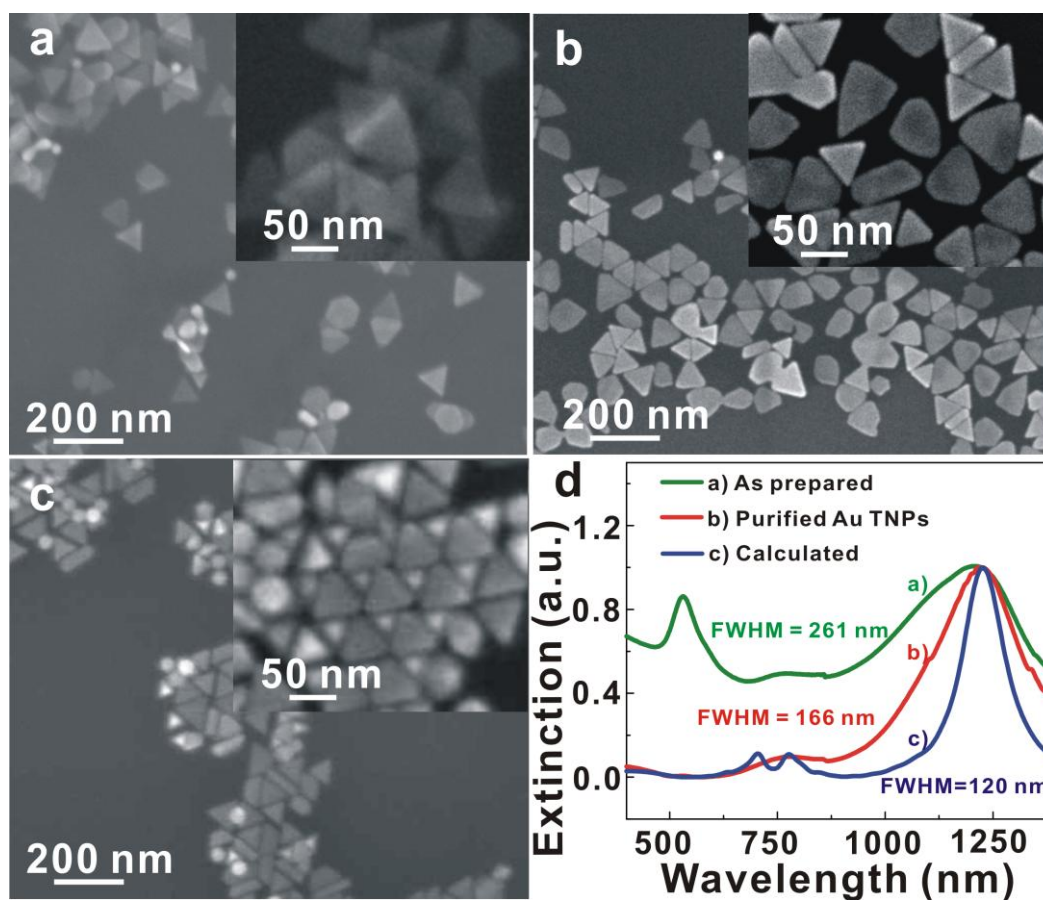


Figure S3. Scanning electron microscopy (SEM) images of the purified Au TNPs with different sizes, and the extinction spectra of the Au TNPs before and after purification. (a-c) SEM images of Au TNPs with diameter of 90, 70, and 40 nm, respectively. (d) The extinction spectra of a) the as-prepared solution and b) the purified Au TNPs, as well as c) the calculated extinction spectrum of a single Au TNP. The full width at half maximum (FWHM) of the purified Au TNPs' extinction curve (red line) is only 166 nm which is nearly 100 nm narrower than that of the as-prepared Au TNP solution. By considering the FWHM of calculated extinction spectrum of a single Au TNP is 120 nm, extinction spectra prove success in our purification of Au TNPs. The extinction peak locating at 535 nm is attributed to the plasmon resonance of Au spherical nanoparticles (green line), and the extinction peaks of 770 and 700 nm are due to the quadrupole and octapole plasmon mode of Au TNPs (bule line).^{1,2}

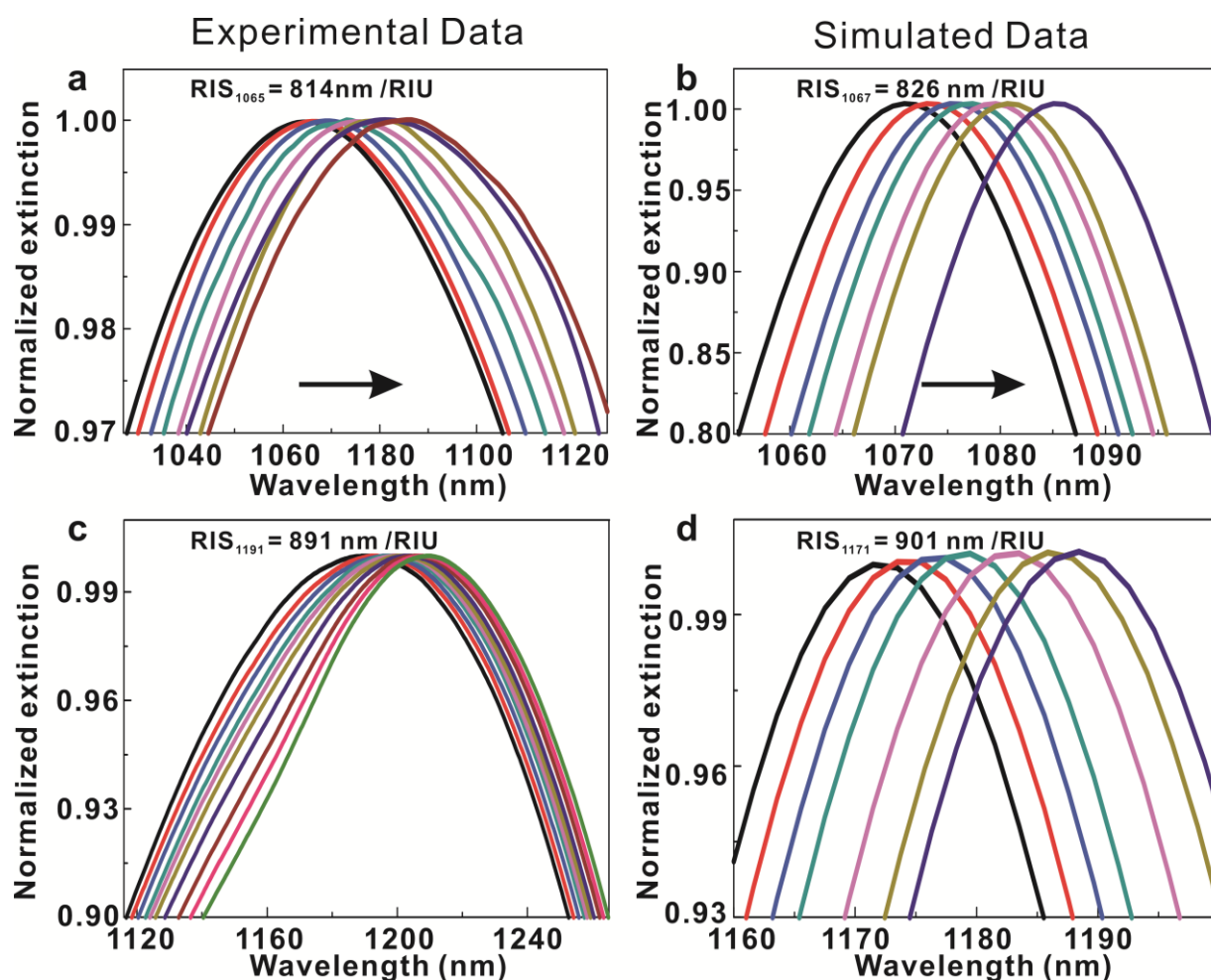


Figure S4. The experimental and COMSOL simulated normalized extinction spectra of the purified Au TNPs in water-glycerol liquid mixtures of varying compositions. The experiment results of Au TNPs with $\lambda_{\text{SPR}} = 1065$ and 1191 nm are shown in (a) and (c), while the

COMSOL simulated data of Au TNPs with $\lambda_{\text{SPR}} = 1067$ and 1171 nm are presented in (b) and (d).

Detailed theoretical considerations of surface area-based purification

Relationships between electrostatic repulsion and particle's surface area. According to the number of Au seed used in our experiment for preparing Au TNPs, one can estimate that the number of Au NPs is $\sim 2.79 \times 10^{12}$ (note that this number is estimated by considering all Au NPs are spheres) in the 45 mL of solution. We can easily calculate that the occupied volume V_{occ} of one NP is $\sim 1.61 \times 10^{-11} \text{ cm}^3$. By taking into account the actual volume ($V_0 = 3.35 \times 10^{-17} \text{ cm}^3$) of the particle, one can determine that the ratio of V_{occ} to V_0 is $\sim 4.83 \times 10^5$; two times of its cube root of (~ 157) reflects the distance between two adjacent nanoparticles, which is ~ 100 times to the size of the NP. Thus, the nanoparticle considered in our mode can be regarded as point charge.

By considering electrostatic repulsion force between two point charges, we derive the total sum of the magnitude for electrostatic repulsion force $F_{c,i} = k\sigma^2 S_i \sum_j (S_j^{\text{TNP}} + S_j^{\text{SNP}})$, $k = \frac{1}{4\pi\epsilon r_{i,j}^2}$ which the particle i applied from its adjacent positive charged NPs (j), where, σ is the surface charge density (we consider that σ is identical for all NPs), S_i is the surface area of the NP (TNP or SNP) i , S^{TNP} and S^{SNP} are surface areas of the TNPs and SNPs, respectively. After adding the anion of Cl^- , σ is reduced; one can easily derive the change rate of $F_{c,i}$ with σ :

$$\frac{\partial F_{c,i}}{\partial \sigma} = 2k\sigma S_i \sum_j (S_j^{\text{TNP}} + S_j^{\text{SNP}}) \quad (1)$$

In any moment when the system is stable, σ and $\sum_j (S_j^{\text{TNP}} + S_j^{\text{SNP}})$ can be viewed as constants,

$\frac{\partial F_{c,i}}{\partial \sigma}$ is then proportional to the particle's surface area S_i . Thus, TNPs with larger surface areas exhibit faster decrease of Coulomb repulsion as it applied along with the decrease of σ ,

which reduces their dispersion ability in CTAB solution to a greater extent than the smaller ones. After the dispersion ability reduced, we next see that the nanostructures with larger surface areas will preferentially assemble into robust crystals by attractive depletion force.

Relationships between attractive depletion force and particle's surface area. Depletion forces are purely entropic in nature and arise when small, nonadsorbing molecules, such as surfactants, are added to a colloidal solution of particles.^[3] Young et al. have calculated the depletion interaction energy for Au TNPs in CTAB solution, as shown in Equation 2:^[4]

$$E_{\text{dep}} = -\Delta\Pi A(t_{\text{plate,eff}} + d_{\text{CTAB,eff}} - d) \quad (2)$$

where, $\Delta\Pi$ is the osmotic pressure difference, A is the area of a triangular nanoplate face, $t_{\text{plate,eff}}$ and $d_{\text{CTAB,eff}}$ are effective sizes of the prisms and CTAB micelles, respectively, d is the center-to-center interparticle spacing between prisms. Similarly, Equation 2 is fully applicable to our Au TNPs and SNPs. By considering that the depletion forces induce Au TNPs assemble into one-dimensional lamellar crystals, the magnitude of attractive depletion force between two adjacent TNPs can be deduced as the following:

$$F_{\text{dep}} = \left| -\frac{\partial E_{\text{dep}}}{\partial d} \right| = \frac{1}{2} \Delta\Pi (t_{\text{TNP,eff}} + d_{\text{CTAB,eff}} - 1) \cdot S^{\text{TNP}} \quad (3)$$

where, $S^{\text{TNP}} \approx 2A$, A is the area of one TNP face. We neglect the lateral areas of Au TNPs due to a very thin thickness of Au TNP. Equation 3 helps us understand why depletion interactions favor the assembly of TNPs: The attractive depletion force of the system is proportional to the surface area of the particles. The TNPs have larger smooth surfaces and feel larger depletion attractions at greater distances compared to those of SNPs. Thus, the nanostructures with larger surface areas will preferentially assemble into one-dimensional lamellar crystals, resulting in a decrease of the effective surface area (and further the electrostatic repulsion) of this lamellar crystal as a whole, which promotes their sedimentation and separation from other NPs. Note here that, we have not listed the magnitude of attractive depletion force between two adjacent SNPs, due to their small smooth surfaces and very weak

depletion attractions.^[4]

Brownian motion discussion. The particle undergoing sedimentation is always kicked another significant force, that is Brownian fluctuating force F_f ,^[5] arising from intense Brownian movement of NPs. Since the nanoparticles suspended in the liquid are very small, Brownian movement of the particles is quite possible and intensive. Brownian particle can be defined as Equation 4:^[6, 7]

$$v_N = \frac{1}{D_N} \sqrt{\frac{18k_B T}{\pi \rho_N D_N}} \quad (4)$$

where k_b is the Boltzmann constant, T the temperature, ρ_N the density, and D_N the diameter of the nanoparticle. The root-mean-square velocity for Au SNPs and TNPs,

$$v_N^{\text{TNP}} = k_1 \cdot (S^{\text{TNP}})^{-\frac{3}{4}}, v_N^{\text{SNP}} = k_2 \cdot (S^{\text{SNP}})^{-\frac{3}{4}} \quad (5)$$

where $k_1 = \left(\frac{\sqrt{3}}{2}\right)^{\frac{3}{4}} \sqrt{\frac{18k_B T}{\pi \rho_N}}$, $k_2 = \pi^{\frac{3}{4}} \sqrt{\frac{18k_B T}{\pi \rho_N}}$, $k_1 < k_2$, $S^{\text{TNP}} \approx 2A^{\text{TNP}}$, $S^{\text{TNP}} > S^{\text{SNP}}$, S^{TNP} and S^{SNP} are

surface areas of Au TNP and SNP, respectively. Note here that, we neglect the lateral areas of Au TNPs. This root-mean-square velocity can reflect the intense degree of Brownian motion and the dispersion ability of the Brownian particles. According to Equation 5, NPs with larger surface area S show a weaker Brownian movement and weaker dispersion ability compared to those of NPs with smaller S , implying that SNP's intense Brownian movement is another favorable factor for Au TNPs separated from SNPs.

From the theoretical discussion above, one can see that the particle's surface area plays a significant role in chemical purification. After the addition of Cl⁻, the electrostatic repulsion between NPs reduces, especially for the NPs with larger surface areas. Along with the further reduce of the dispersion ability caused by the depletion assembling and the relative weaker Brownian motion, the nanostructures with the larger surface areas preferentially precipitate and are separated from the ones with smaller surface areas.

References

1. J. E. Millstone, S. Park, K. L. Shuford, L. Qin, G. C. Schatz and C. A. Mirkin, *J. Am. Chem. Soc.*, 2005, **127**, 5312.
2. Z. Li, Y. Yu, Z. Chen, T. Liu, Z. K. Zhou, J. B. Han, J. Li, C. Jin and X. H. Wang, *J. Phys. Chem. C*, 2013, **117**, 20127.
3. S. Asakura and F. Oosawa, *J. Chem. Phys.*, 1954, **22**, 1255.
4. K. L. Young, M. R. Jones, J. Zhang, R. J. Macfarlane, R. Esquivel-Sirvent, R. J. Nape, J. Wu, G. C. Schatz, B. Lee and C. A. Mirkin, *Proc. Natl. Acad. Sci. USA*, 2012, **109**, 2240.
5. V. Sharma, K. Park and M. Srinivasarao, *Proc. Natl. Acad. Sci. USA*, 2009, **106**, 4981.
6. D. A. McQuarrie, *Statistical Mechanics* (Viva Books Private Ltd., New Delhi, **1981**).
7. R. Prasher, *Phys Rev Lett.*, 2005, **94**, 025901.